Applied Numerical Mathematics 119 (2017) 179–193

Contents lists available at ScienceDirect

Applied Numerical Mathematics

www.elsevier.com/locate/apnum

A second order operator splitting numerical scheme for the "good" Boussinesq equation

Cheng Zhang [a], Hui Wang [a], Jingfang Huang [b], Cheng Wang [c,*], Xingye Yue [a]

[a] School of Mathematical Sciences, Soochow University, Suzhou 215006, PR China
[b] Department of Mathematics, University of North Carolina, Chapel Hill, NC 27599, USA
[c] Mathematics Department, University of Massachusetts, North Dartmouth, MA 02747, USA

ARTICLE INFO

Article history:
Received 12 July 2016
Received in revised form 12 February 2017
Accepted 19 April 2017
Available online 27 April 2017

Keywords:
"good" Boussinesq equation
Operator splitting
Fourier pseudo-spectral method
Aliasing error
Stability and convergence analysis

ABSTRACT

The nonlinear stability and convergence analyses are presented for a second order operator splitting scheme applied to the "good" Boussinesq equation, coupled with the Fourier pseudo-spectral approximation in space. Due to the wave equation nature of the model, we have to rewrite it as a system of two equations, for the original variable u and $v = u_t$, respectively. In turn, the second order operator splitting method could be efficiently designed. A careful Taylor expansion indicates the second order truncation error of such a splitting approximation, and a linearized stability analysis for the numerical error function yields the desired convergence estimate in the energy norm. In more details, the convergence in the energy norm leads to an $\ell^\infty(0, T^*; H^2)$ convergence for the numerical solution u and $\ell^\infty(0, T^*; \ell^2)$ convergence for $v = u_t$. And also, the presented convergence is unconditional for the time step in terms of the spatial grid size, in comparison with a severe time step restriction, $\Delta t \le Ch^2$, required in many existing works.

1. Introduction

In this article we study a commonly used soliton-producing nonlinear wave equation, the so-called "good" Boussinesq (GB) equation:

$$u_{tt} = -u_{xxxx} + u_{xx} + (u^p)_{xx}, \quad \text{with an integer } p \ge 2. \tag{1.1}$$

In comparison with the well-known Korteweg–de Vries (KdV) equation, the wave equation form of (1.1) introduces the second order temporal derivative. The GB equation and its various extensions have been extensively analyzed in the existing literature, such as a closed form solution for the two soliton interaction in [46], a highly complicated mechanism for the solitary waves interaction in [47], and the nonlinear stability and convergence of some simple finite difference schemes in [49]. Many other analytical and numerical works related to GB equations could also be found, for example, in [1,8,7,14, 15,25,16,37,48,50,58].

For simplicity, a periodic boundary condition over a 1-D domain $\Omega = (0, L)$ is considered in this article. This L-periodicity assumption is reasonable, since the solution to (1.1) decays exponentially outside $[0, L]$ over a finite time interval $(0, T)$. Because of the assumed periodic boundary condition, the Fourier collocation (pseudo-spectral) formulation turns out to be

* Corresponding author.
E-mail address: cwang1@umassd.edu (C. Wang).

http://dx.doi.org/10.1016/j.apnum.2017.04.006
0168-9274/

a natural choice to obtain the optimal spatial accuracy. The development of spectral and pseudo-spectral schemes has had a long history. At the theoretical side, the stability analysis for linear time-dependent problems has been available in [26,45], etc, based on eigenvalue estimates. For the nonlinear problems, the readers are referred to the pioneering works by Maday and Quarteroni [40–42] for steady-state spectral solutions. Many more numerical analysis works for nonlinear equations have been reported since then, such as [12,29,44,55,56] for one-dimensional conservation laws, [21,22] for semi-discrete viscous Burgers' and Navier–Stokes equations, [19,28,30] for the Galerkin spectral method to the Navier–Stokes equations, [9,27] for the fully discrete method applied to viscous Burgers' equation, [43,52] for the Korteweg–de Vries equation, and [17,18] for the Benjamin–Ono equation or related non-local models, etc.

For the GB equation (1.1), we like to review a related work of the nonlinear stability and convergence analysis for the pseudo-spectral schemes. In [16], a second order temporal discretization was proposed and analyzed, and a full order convergence was proved in a weak energy norm: an L^2 norm of u combined with an H^{-2} norm of $v = u_t$. This energy norm is much weaker than the one reported in [38], where the linear part was analyzed: an H^2 norm of u combined with an L^2 norm of $v = u_t$. Such a theoretical weakness turns out to be a technical issue, due to the lack of a useful tool to control the discrete L^2 norm of the nonlinear error term, associated with $(u^p)_{xx}$, in the pseudo-spectral space. Moreover, due to certain technical difficulties, a severe time step restriction: $\Delta t \le Ch^2$ (with C a fixed constant), had to be imposed in the earlier analysis work [16].

In this article, we propose and analyze a second order operator splitting scheme applied to the GB equation (1.1). There have been many existing works of operator splitting numerical approximation to nonlinear PDEs, such as [3,39,53,57] for the nonlinear Schrödinger equation, [2] for the incompressible magnetohydrodynamics system, [4,5] for the delay equation, [23] for the nonlinear evolution equation, [24] for the Vlasov-type equation, [33] for a generalized Leland's mode, [34] for Allen–Cahn equation, [36] for the molecular beamer epitaxy (MBE) equation, [62] for nonlinear solvation problem, etc. On the other hand, a theoretical analysis for the nonlinear operator scheme turns out to be very challenging, due to its multi-stage nature. Among the above-mentioned references, the second order and higher order convergence analyses for the nonlinear Schrödinger equation, given by [39,57], respectively, are worthy of discussion. In these two theoretical works, the authors made use of the special form of the nonlinear term appearing in the Gross–Pitaevskii model, so that an unconditional stability estimate is available, and the desired convergence result could be derived in an appropriate way. A similar idea was applied in Shen [53] to obtain the second order (in time) convergence for the Gross–Pitaevskii equation, in conjunction with Hermite collocation spectral accuracy in space. And also, a second order convergence analysis [36] for the operator splitting applied to the MBE equation is very interesting.

Meanwhile, it is observed that, all these existing operator splitting numerical schemes were applied to equations involved with only the first order temporal derivative. For a nonlinear wave equation in which a second order temporal derivative appears, such as the GB equation (1.1), there has been no theoretical analysis for the operator splitting approach. To overcome this difficulty, we have to rewrite this equation into the following system:

$$u_t = v, \tag{1.2}$$

$$v_t = -u_{xxxx} + u_{xx} + (u^p)_{xx}. \tag{1.3}$$

By setting $\boldsymbol{u} = (u, v)^T$, the above first order system is reformulated as

$$\boldsymbol{u}_t = \mathcal{L}\boldsymbol{u} + F(\boldsymbol{u}), \ \text{with} \ \mathcal{L}\boldsymbol{u} = \begin{pmatrix} v \\ -u_{xxxx} + u_{xx} \end{pmatrix}, \ F(\boldsymbol{u}) = \begin{pmatrix} 0 \\ (u^p)_{xx} \end{pmatrix}. \tag{1.4}$$

Based on this equivalent reformulation, we are able to derive the second order Strang splitting in three stages. It is remarkable that the both the linear wave equation and nonlinear stages could be exactly updated. In particular, the exact solver for the nonlinear stage becomes available due to the fact that the nonlinear term turns out to be a constant, which comes from the splitting form of (1.2)–(1.3). In addition, a detailed Taylor expansion indicates a full second order accurate temporal truncation error, combined with the spectral accuracy in space. And also, we introduce a discrete energy norm similar to [38], and a careful linearized stability analysis for the numerical error function yields the desired convergence result in the energy norm: an H^2 convergence of u combined with an L^2 convergence of $v = u_t$, with the full order convergence rate in both time and space.

In particular, we directly analyze the numerical error associated with the nonlinear error term $D_N^2(u^p)$, with the help of aliasing error control technique in the pseudo-spectral space developed in [27]. In the nonlinear error estimate, we set an a-priori H^2 assumption of the numerical error at the previous time steps, and a careful analysis indicates an H^2 convergence result at the next time step, based on the L^∞ and H^2 bound of the numerical solution. In turn, these bounds could be obtained at the next time step, because of the H^2 error estimate and the corresponding Sobolev embedding. Therefore, the inverse inequality in the stability analysis is not needed and any scaling law between Δt and h is avoided, compared with the $\Delta t \le Ch^2$ constraint reported in [16].

This paper is outlined as follows. In Section 2 we review the Fourier pseudo-spectral formulation, and an aliasing error control lemma (proved in [27]). In Section 3 we present the second order (in time) operator splitting scheme for the GB equation (1.1), with the Fourier pseudo-spectral approximation in space. The detailed consistency analysis is studied in Section 4, and the stability and convergence analysis is reported in Section 5. The numerical results are presented in Section 6. Finally, some concluding remarks are made in Section 7.

2. Review of Fourier spectral and pseudo-spectral approximations

For any $f(x) \in L^2(\Omega)$, $\Omega = (0, L)$, its Fourier series are formulated as

$$f(x) = \sum_{l=-\infty}^{\infty} \hat{f}_l e^{2\pi i l x/L}, \quad \text{with} \quad \hat{f}_l = \int_{\Omega} f(x) e^{-2\pi i l x/L} dx. \tag{2.5}$$

In turn, the projection of $f(x)$ onto $\mathcal{B}^N$, the space of trigonometric polynomials in x of degree up to N, becomes

$$\mathcal{P}_N f(x) = \sum_{l=-N}^{N} \hat{f}_l e^{2\pi i l x/L}. \tag{2.6}$$

In the practical computations, a pseudo-spectral approximation at a given set of points is more preferred, due to the computational efficiency. To obtain such a pseudo-spectral approximation, an interpolation operator $\mathcal{I}_N$ has to be introduced. Given a uniform numerical grid with $(2N+1)$ points and a discrete vector function $\mathbf{f}$ where $\mathbf{f}_j = f(x_j)$, $0 \le j \le 2N$, the $(2N+1)$ pseudo-spectral coefficients $(\hat{f}_c^N)_l$ could be computed based on the interpolation condition $f(x_i) = (\mathcal{I}_N f)(x_i)$, over the $2N+1$ equidistant points [6,11,31]:

$$(\hat{f}_c^N)_l = h \sum_{j=0}^{2N} \mathbf{f}_j e^{-2\pi i l x_j/L}, \quad \text{with } \mathbf{f}_j = f(x_j), h = \tfrac{L}{2N+1}, \quad \forall -N \le l \le N. \tag{2.7}$$

In turn, the Fourier interpolation of the periodic function f is defined as

$$(\mathcal{I}_N f)(x) = \sum_{l=-N}^{N} (\hat{f}_c^N)_l e^{2\pi i l x/L}. \tag{2.8}$$

It is well-known that an efficient algorithm using the fast Fourier transform (FFT) is available to compute the collocation coefficients given by (2.7). In general, the pseudo-spectral coefficients may not be equal to the actual Fourier coefficients, due to the appearance of the aliasing error. In other words, $\mathcal{P}_N f(x) \ne \mathcal{I}_N f(x)$, and $\mathcal{P}_N f(x_i) \ne \mathcal{I}_N f(x_i)$, except in the case that $f \in \mathcal{B}^N$; see [54] for more details.

Based on the interpolation formula (2.8), one can easily take derivative by simply multiplying the appropriate Fourier coefficients $(\hat{f}_c^N)_l$ by $2l\pi i/L$. Moreover, the higher order derivatives could be computed in the same way, so that differentiation in physical space is accomplished via multiplication in Fourier space. As long as f and all its derivatives (up to m-th order) are continuous and periodic on Ω, the convergence of the derivatives of the projection and interpolation is given by

$$\begin{aligned} &\|\partial^k f(x) - \partial^k \mathcal{P}_N f(x)\| \le C \|f^{(m)}\| h^{m-k}, \quad \text{for } 0 \le k \le m, \\ &\|\partial^k f(x) - \partial^k \mathcal{I}_N f(x)\| \le C \|f\|_{H^m} h^{m-k}, \quad \text{for } 0 \le k \le m,\ m > \frac{d}{2}, \end{aligned} \tag{2.9}$$

in which $\|\cdot\|$ denotes the L^2 norm. The more detailed discussions of approximation theory could be found in [10] by Canuto and Quarteroni.

For any periodic function f, we denote its collocation approximation as

$$f(x_j) = (\mathcal{I}_N f)_i = \sum_{l=-N}^{N} (\hat{f}_c^N)_l e^{2\pi i l x_j}, \quad \forall 0 \le j \le 2N. \tag{2.10}$$

In turn, the discrete differentiation operator $\mathcal{D}_N$ could be defined on the vector of grid values $\mathbf{f} = f(x_j)$, $0 \le j \le 2N$. In more details, the collocation coefficients $(\hat{f_c^N})_l$ are computed via FFT, as given by (2.7), and one could multiply them by the corresponding eigenvalues (given by $2l\pi i$) and perform the inverse FFT. Of course the differentiation operator $\mathcal{D}_N$ could be viewed as a matrix, so that the pseudo-spectral differentiation process becomes a matrix–vector multiplication. The same process is performed for the second and fourth derivatives ∂_x^2, ∂_x^4, with the collocation coefficients multiplied by $(-4\pi^2 l^2/L^2)$ and $(16\pi^4 l^4/L^4)$, respectively. In turn, the differentiation matrix can be applied for multiple times, i.e. the vector $\mathbf{f}$ is multiplied by $\mathcal{D}_N^2$ and $\mathcal{D}_N^4$, respectively.

Since the pseudo-spectral differentiation is taken at a point-wise level, a discrete L^2 norm and inner product need to be introduced to facilitate the analysis. Given any periodic grid functions $\mathbf{f}$ and $\mathbf{g}$ (over the numerical grid), the discrete L^2 inner product and norm are defined as

$$\|\mathbf{f}\|_2 = \sqrt{\langle \mathbf{f}, \mathbf{f} \rangle}, \quad \text{with} \quad \langle \mathbf{f}, \mathbf{g} \rangle = \frac{1}{2N+1} \sum_{i=0}^{2N} \mathbf{f}_i \mathbf{g}_i. \tag{2.11}$$

The following summation by parts formulas are valid (see [13,27]):

$$\langle \mathbf{f}, \mathcal{D}_N \mathbf{g} \rangle = -\langle \mathcal{D}_N \mathbf{f}, \mathbf{g} \rangle, \quad \left\langle \mathbf{f}, \mathcal{D}_N^2 \mathbf{g} \right\rangle = -\langle \mathcal{D}_N \mathbf{f}, \mathcal{D}_N \mathbf{g} \rangle, \quad \left\langle \mathbf{f}, \mathcal{D}_N^4 \mathbf{g} \right\rangle = \left\langle \mathcal{D}_N^2 \mathbf{f}, \mathcal{D}_N^2 \mathbf{g} \right\rangle. \tag{2.12}$$

In addition, an aliasing error control estimate in Fourier pseudo-spectral approximation, established in [27], is necessary for the nonlinear analysis. For any function $\varphi(x)$ in the space $\mathcal{B}^{pN}$, its collocation coefficients $\hat{q}_l^N$ are computed based on the $2N+1$ equidistant points. In turn, $\mathcal{I}_N\varphi(x)$ is given by the continuous expansion based on these coefficients:

$$\mathcal{I}_N\varphi(x) = \sum_{l=-N}^{N} \hat{q}_l^N \mathrm{e}^{2\pi \mathrm{i} l x/L}. \tag{2.13}$$

Note that the interpolation operator $\mathcal{I}_N$ maps a periodic function into another periodic function: the computation formula (2.7) for the discrete Fourier coefficients is based on the periodic grid function $\mathbf{f}$, the interpolation value of the continuous function f, while formula (2.8) maps f to a periodic function in $\mathcal{B}^N$. Since $\varphi(x) \in \mathcal{B}^{pN}$, we conclude that $\mathcal{I}_N\varphi(x) \neq \mathcal{P}_N\varphi(x)$ due to the aliasing error.

This following estimate is able to bound the aliasing error for the nonlinear term, which will play a critical role in the numerical analysis; the detailed proof can be found in [27].

Lemma 2.1. *For any $\varphi \in \mathcal{B}^{pN}$ (with p an integer) in dimension d, we have*

$$\|\mathcal{I}_N\varphi\|_{H^k} \leq \left(\sqrt{p}\right)^d \|\varphi\|_{H^k}. \tag{2.14}$$

3. The second order operator splitting scheme

Following the second order Strang splitting formula $\boldsymbol{u}^{n+1} = \mathrm{e}^{\frac{1}{2}\Delta t F} \mathrm{e}^{\Delta t \mathcal{L}} \mathrm{e}^{\frac{1}{2}\Delta t F} \boldsymbol{u}^n$, we formulate the splitting scheme for the GB equation (1.4) as: given (u^n, v^n), the numerical solution (u^{n+1}, v^{n+1}) is obtained through the following three stages.

Stage 1: nonlinear part: linear advance for v, with $\frac{1}{2}\Delta t$ advance

$$\partial_t u_1 = 0, \quad \text{over } (t^n, t^{n+1/2}), \tag{3.15}$$

$$\partial_t v_1 = D_N^2((u_1)^p), \quad \text{over } (t^n, t^{n+1/2}), \tag{3.16}$$

$$u_1(t^n) = u^n, \quad v_1(t^n) = v^n. \tag{3.17}$$

The key point for this stage is that, $D_N^2((u_1)^p)$ becomes a constant (in time) term in (3.16), due to the splitting form (1.4). In more details, we denote $u^{n,(1)} = u_1(t^{n+1/2})$, $v^{n,(1)} = v_1(t^{n+1/2})$, and the numerical solutions are explicitly given by

$$u^{n,(1)} = u^n, \quad v^{n,(1)} = v^n + \frac{1}{2}\Delta t D_N^2\left((u^n)^p\right). \tag{3.18}$$

Stage 2: linear wave equation, with Δt advance

$$\partial_t u_2 = v_2, \quad \text{over } (t^n, t^{n+1}), \tag{3.19}$$

$$\partial_t v_2 = -D_N^4 u_2 + D_N^2 u_2, \quad \text{over } (t^n, t^{n+1}), \tag{3.20}$$

$$u_2(t^n) = u^{n,(1)}, \quad v_2(t^n) = v^{n,(1)}. \tag{3.21}$$

We denote $u^{n*} = u_2(t^{n+1})$, $v^{n*} = v_2(t^{n+1})$. Clearly u_2 satisfies the linear wave equation

$$\partial_t^2 u_2 = -D_N^4 u_2 + D_N^2 u_2, \quad \text{over } (t^n, t^{n+1}), \tag{3.22}$$

$$u_2(t^n) = u^{n,(1)}, \quad \partial_t u_2(t^n) = v^{n,(1)}, \tag{3.23}$$

and this wave equation could be exactly solved via FFT over the 1-D domain $\Omega = (0, L)$.

Stage 3: nonlinear part: linear advance for v, with $\frac{1}{2}\Delta t$ advance

$$\partial_t u_3 = 0, \quad \text{over } (t^n, t^{n+1/2}), \tag{3.24}$$

$$\partial_t v_3 = D_N^2((u_3)^p), \quad \text{over } (t^n, t^{n+1/2}), \tag{3.25}$$

$$u_3(t^n) = u^{n*}, \quad v_3(t^n) = v^{n*}. \tag{3.26}$$

We denote $u^{n+1} = u_3(t^{n+1/2})$, $v^{n+1} = v_3(t^{n+1/2})$. Similar to the first stage, the numerical solutions are explicitly given by

$$u^{n+1} = u^{n*}, \quad v^{n+1} = v^{n*} + \frac{1}{2}\Delta t D_N^2\left((u^{n*})^p\right). \tag{3.27}$$

We recall that the exact solution u_e to the GB equation (1.1) is mass conservative, provided that $v^0(x) = u_t(x, t=0) \equiv 0$:

$$\int_\Omega u_e(\cdot, t)\, dx \equiv \int_\Omega u_e(\cdot, 0)\, dx := \bar{C}_0, \quad \text{with} \quad \forall t > 0. \tag{3.28}$$

Meanwhile, such a property is also valid for the proposed operator splitting scheme, at a discrete level; see the following lemma.

Lemma 3.1. *The numerical scheme (3.15)–(3.26) is mass conservative at the discrete level, provided that* $v^0 \equiv 0$*:*

$$\overline{u^k} := h\sum_{i=0}^{N-1} u_i^k \equiv \overline{u^0} = \beta_0, \quad \forall k \geq 0. \tag{3.29}$$

Proof. The solution formula (3.18) implies the mass conservation in the first stage:

$$\overline{u^{n,(1)}} = \overline{u^n}, \quad \overline{v^{n,(1)}} = \overline{v^n} = 0, \quad \text{since } \overline{D_N^2\left((u^n)^p\right)} = 0. \tag{3.30}$$

In addition, a discrete summation of the linear wave equation (3.22) gives

$$\partial_t^2 \overline{u_2} = 0, \quad \text{since } \overline{D_N^4 u_2} = 0,\ \overline{D_N^2 u_2} = 0. \tag{3.31}$$

Its combination with the initial condition:

$$\overline{\partial_t u_2(t^n)} = \overline{v_2(t^n)} = \overline{v^{n,(1)}} = 0, \tag{3.32}$$

yields the mass conservation of the second stage:

$$\overline{u^{n*}} = \overline{u_2(t^{n+1})} = \overline{u_2(t^n)} = \overline{u^{n,(1)}}, \quad \overline{v^{n*}} = \overline{v_2(t^{n+1})} = \overline{v_2(t^n)} = \overline{v^{n,(1)}} = 0. \tag{3.33}$$

Similar to the first stage, the solution formula (3.27) indicates the following mass conservation:

$$\overline{u^{n+1}} = \overline{u^{n*}}, \quad \overline{v^{n+1}} = \overline{v^{n*}} = 0, \quad \text{since } \overline{D_N^2\left((u^{n*})^p\right)} = 0. \tag{3.34}$$

Finally, a combination of (3.30), (3.33) and (3.34) leads to

$$\overline{u^{n+1}} = \overline{u^n}, \quad \overline{v^{n+1}} = \overline{v^n} = 0, \tag{3.35}$$

which in turn implies the mass conservation identity (3.29). □

Remark 3.2. For many nonlinear wave equations, there are certain invariant quantities, which are constant physical quantities in time. For example, for the generalized classical Korteweg–de Vries (GKDV) equation

$$u_t + (u^p)_x + \varepsilon u_{xxx} = 0, \quad \text{with an integer } p \geq 2. \tag{3.36}$$

There are two invariant quantities, namely the mass and the kinematics energy invariants:

$$I_{1,KDV} = \int_\Omega u(x)\, dx, \quad I_{2,KDV} = \int_\Omega u^2(x)\, dx. \tag{3.37}$$

In a recent work [32], local discontinuous Galerkin (LDG) methods were applied to the GKDV equation (3.36) and analyzed in details. In particular, the conservative property for the two invariant quantities was proved for the semi-discrete LDG method (keeping time continuous), and a posteriori error estimate was provided. Also see the related works [35,59–61] for the LDG methods applied to the KDV-type equations.

The GB equation (1.1) could be viewed as a traveling wave solution of (3.36) in a special form [51]. There are also two invariant quantities for this model, namely the mass and the functional energy invariants:

$$I_{1,GB} = \int_\Omega u(x)\, dx, \quad I_{2,GB} = \frac{1}{2}\|u_t\|_{H^{-1}}^2 + \int_\Omega \left(\frac{1}{p+1}u^{p+1} + \frac{1}{2}u^2 + \frac{1}{2}u_x^2\right) dx. \tag{3.38}$$

Our proposed numerical scheme (3.15)–(3.26) preserves the mass invariant, as shown by Lemma 3.1. Regarding the second invariant quantity $I_{2,GB}$, the semi-discrete version of (3.15)–(3.26) (i.e., by skipping the temporal discretization) also preserves this invariant. For the fully discrete scheme (3.15)–(3.26), such a conservation could not be justified at a theoretical level, due to the explicit treatment of the nonlinear term.

On the other hand, the convergence analysis (as given by Theorem 3.3) implies that, although an exact conservation of the functional energy invariant $I_{2,GB}$ is not available, we are able to obtain an approximate conservation for the fully discrete scheme. The reason comes from the fact that, the exact solution preserves such a conservation, while an $O(\Delta t^2 + h^m)$ convergence is valid for the proposed numerical scheme, local in time, with H^2 norm for u and L^2 norm for $v = u_t$. A careful calculation indicates such an approximate conservation.

For the linear wave equation (3.22)–(3.23) in the second stage, we have the following identity, by taking an L^2 inner product with $v_2 = \partial_t u_2$:

$$\frac{1}{2}\frac{d}{dt}\|v_2(t)\|_2^2 + \frac{1}{2}\frac{d}{dt}\left(\|D_N u_2(t)\|_2^2 + \|D_N^2 u_2(t)\|_2^2\right) = 0, \quad \forall t^n \le t \le t^{n+1}, \tag{3.39}$$

with the summation by parts formulas (2.12) repeatedly applied. As a result, the following energy conservation is available, since $u^{n*} = u_2(t^{n+1})$, $v^{n*} = v_2(t^{n+1})$:

$$\left\|(u^{n*}, v^{n*})\right\|_E^2 = \left\|(u^{n,(1)}, v^{n,(1)})\right\|_E^2, \quad \text{with} \quad \|(u,v)\|_E^2 = \|D_N u\|_2^2 + \left\|D_N^2 u\right\|_2^2 + \|v\|_2^2. \tag{3.40}$$

Note that the numerical solution (u, v) of (3.15)–(3.26) is a vector function evaluated at discrete grid points. Before the convergence statement of the numerical scheme, its continuous extension in space is introduced, defined by $u^k_{\Delta t,h} = u^k_N$, $v^k_{\Delta t,h} = v^k_N$, in which $u^k_N, v^k_N \in \mathcal{B}^N, \forall k$, are the continuous version of the discrete grid functions u^k, v^k, with the interpolation formula given by (2.10).

The main theoretical result of this article is given by the following theorem.

Theorem 3.3. *For any final time $T^* > 0$, assume the exact solution u_e to the GB equation (1.1) is smooth enough. Denote $u_{\Delta t,h}$, $v_{\Delta t,h}$ as the continuous (in space) extension of the fully discrete numerical solution given by scheme (3.15)–(3.26). As $\Delta t, h \to 0$, the following convergence result is valid:*

$$\left\|u_{\Delta t,h} - u_e\right\|_{\ell^\infty(0,T^*;H^2)} + \left\|v_{\Delta t,h} - v_e\right\|_{\ell^\infty(0,T^*;L^2)} \le C\left(\Delta t^2 + h^m\right), \tag{3.41}$$

provided that the time step Δt and the space grid size h are bounded by given constants which are only dependent on the exact solution. Note that the convergence constant in (3.41) also depends on the exact solution as well as T^*.

4. Consistency analysis

We denote $U^k = u_e(t^k)$, $V^k = v_e(t^k) = \partial_t u_e(t^k)$, for any $k \ge 0$. A detailed Taylor expansion for u_e (up to the third order) at time step t^n gives

$$\begin{aligned} U^{n+1} &= u_e(t^{n+1}) = u_e(t^n) + \Delta t \partial_t u_e(t^n) + \frac{\Delta t^2}{2}\partial_t^2 u_e(t^n) + \frac{\Delta t^3}{6}\partial_t^3 u_e(t^n) + O(\Delta t^4) \\ &= U^n + \Delta t V^n + \frac{\Delta t^2}{2}\left(-U^n_{xxxx} + U^n_{xx} + ((U^n)^p)_{xx}\right) + \frac{\Delta t^3}{6}\left(-V^n_{xxxx} + V^n_{xx} + \mathcal{NL}^n_3\right) + O(\Delta t^4), \\ &\quad \text{with } \mathcal{NL}^n_3 = \left(p(U^n)^{p-1}V^n\right)_{xx}, \end{aligned} \tag{4.1}$$

in which the original GB equation (1.1) was applied. Similarly, the Taylor expansion for v_e at time step t^n gives

$$\begin{aligned} V^{n+1} &= v_e(t^{n+1}) = v_e(t^n) + \Delta t \partial_t v_e(t^n) + \frac{\Delta t^2}{2}\partial_t^2 v_e(t^n) + O(\Delta t^3) \\ &= v_e(t^n) + \Delta t \partial_t^2 u_e(t^n) + \frac{\Delta t^2}{2}\partial_t^3 u_e(t^n) + O(\Delta t^3) \\ &= V^n + \Delta t\left(-U^n_{xxxx} + U^n_{xx} + ((U^n)^p)_{xx}\right) + \frac{\Delta t^2}{2}\left(-V^n_{xxxx} + V^n_{xx} + \mathcal{NL}^n_3\right) + O(\Delta t^3). \end{aligned} \tag{4.2}$$

On the other hand, we denote the following intermediate, approximate solution, in the first stage, analogous to (3.18), at the numerical grid points:

$$U^{n,(1)} = U^n, \quad V^{n,(1)} = V^n + \frac{1}{2}\Delta t D_N^2\left((U^n)^p\right). \tag{4.3}$$

Subsequently, U^{n*}, V^{n*} is defined as the solution of the linear wave equation (3.19)–(3.21) at time instant t^{n+1}, with initial data $U^{n,(1)}$, $V^{n,(1)}$, respectively. In more detail, U_2, V_2 are the solutions of the following O.D.E. system

$$\partial_t U_2 = V_2, \quad \text{over } (t^n, t^{n+1}), \tag{4.4}$$

$$\partial_t V_2 = -D_N^4 U_2 + D_N^2 U_2, \quad \text{over } (t^n, t^{n+1}), \tag{4.5}$$

$$U_2(t^n) = U^{n,(1)}, \quad V_2(t^n) = V^{n,(1)}, \tag{4.6}$$

and $U^{n*} = U_2(t^{n+1})$, $V^{n*} = V_2(t^{n+1})$. Similar Taylor expansions for U_2 and V_2 (in time) imply that

$$\begin{aligned} U^{n*} &= U_2(t^{n+1}) = U_2(t^n) + \Delta t \partial_t U_2(t^n) + \frac{\Delta t^2}{2} \partial_t^2 U_2(t^n) + O(\Delta t^3) \\ &= U^n + \Delta t V^{n,(1)} + \frac{\Delta t^2}{2} \left(-D_N^4 U^n + D_N^2 U^n \right) + O(\Delta t^3) \\ &= U^n + \Delta t V^n + \frac{\Delta t^2}{2} \left(-D_N^4 U^n + D_N^2 U^n + D_N^2 \left((U^n)^p \right) \right) + O(\Delta t^3), \end{aligned} \tag{4.7}$$

$$\begin{aligned} V^{n*} &= V_2(t^{n+1}) = V_2(t^n) + \Delta t \partial_t V_2(t^n) + \frac{\Delta t^2}{2} \partial_t^2 V_2(t^n) + O(\Delta t^3) \\ &= V^{n,(1)} + \Delta t \left(-D_N^4 U^n + D_N^2 U^n \right) + \frac{\Delta t^2}{2} \left(-D_N^4 V^{n,(1)} + D_N^2 V^{n,(1)} \right) + O(\Delta t^3) \\ &= V^n + \Delta t \left(-D_N^4 U^n + D_N^2 U^n + \frac{1}{2} D_N^2 ((U^n)^p) \right) \\ &\quad + \frac{\Delta t^2}{2} \left(-D_N^4 V^n + D_N^2 V^n \right) + O(\Delta t^3), \end{aligned} \tag{4.8}$$

in which the numerical approximation (4.3) has been repeatedly applied in the derivation.

Next, we denote the approximate solution $(U^{n,(3)}, V^{n,(3)})$ as

$$U^{n,(3)} = U^{n*}, \quad V^{n,(3)} = V^{n*} + \frac{1}{2} \Delta t D_N^2 \left((U^{n*})^p \right), \tag{4.9}$$

analogous to the numerical scheme (3.27) in the third stage. A careful comparison between $U^{n,(3)}$ and U^{n+1} shows that

$$U^{n+1} - U^{n,(3)} = U^{n+1} - U^{n*} = O(\Delta t^3 + \Delta t h^m), \tag{4.10}$$

in which the Taylor expansions (4.1) and (4.7) were recalled, and the pseudo-spectral approximation estimate (2.9) was used. For the comparison between $V^{n,(3)}$ and V^{n+1}, we observe that

$$(U^{n*})^p = \left(U^n + \Delta t V^n \right)^p + O(\Delta t^2) = (U^n)^p + p \Delta t (U^n)^{p-1} V^n + O(\Delta t^2). \tag{4.11}$$

This in turn implies that

$$\begin{aligned} V^{n,(3)} &= V^{n*} + \frac{1}{2} \Delta t D_N^2 \left((U^{n*})^p \right) \\ &= V^n + \Delta t \left(-D_N^4 U^n + D_N^2 U^n + \frac{1}{2} D_N^2 ((U^n)^p) \right) + \frac{\Delta t^2}{2} \left(-D_N^4 V^n + D_N^2 V^n \right) \\ &\quad + \frac{1}{2} \Delta t D_N^2 (U^n)^p) + \frac{\Delta t^2}{2} D_N^2 \left(p (U^n)^{p-1} V^n \right) + O(\Delta t^3) \\ &= V^n + \Delta t \left(-D_N^4 U^n + D_N^2 U^n + D_N^2 ((U^n)^p) \right) \\ &\quad + \frac{\Delta t^2}{2} \left(-D_N^4 V^n + D_N^2 V^n + D_N^2 \left(p (U^n)^{p-1} V^n \right) \right) + O(\Delta t^3). \end{aligned} \tag{4.12}$$

Therefore, the following approximation is available

$$V^{n+1} - V^{n,(3)} = O(\Delta t^3 + \Delta t h^m), \tag{4.13}$$

based on a comparison between (4.2) and (4.12), combined with the pseudo-spectral approximation estimate (2.9).

Note that the consistency estimates (4.10) and (4.13) could be rewritten as

$$\frac{U^{n+1}-U^{n*}}{\Delta t}=\tau_1^n, \tag{4.14}$$

$$\frac{V^{n+1}-V^{n*}}{\Delta t}=\frac{1}{2}D_N^2((U^{n*})^p)+\tau_2^n, \tag{4.15}$$

in which $\|\tau_1^n\|_{H_h^2}$, $\|\tau_2\|_2\le C_0(\Delta t^2+h^m)$, with the $\|\cdot\|_{H_h^2}$ norm introduced as

$$\|f\|_{H_h^2}^2=\|f\|_2^2+\|D_N f\|_2^2+\|D_N^2 f\|_2^2. \tag{4.16}$$

5. Stability and convergence analysis

The point-wise numerical error grid functions are given by

$$\tilde{u}^k=U^k-u^k,\quad \tilde{v}^k=V^k-v^k,\quad \tilde{u}^{k*}=U^{k*}-u^{k*},\quad \tilde{v}^{k*}=V^{k*}-v^{k*}, \tag{5.17}$$

$$\tilde{u}^{k,(1)}=U^{k,(1)}-u^{k,(1)},\quad \tilde{v}^{k,(1)}=V^{k,(1)}-v^{k,(1)}. \tag{5.18}$$

In addition, the following auxiliary error functions are defined

$$\tilde{u}_1=U_1-u_1,\quad \tilde{v}_1=V_1-v_1,\quad \tilde{u}_2=U_2-u_2,\quad \tilde{v}_2=V_2-v_2. \tag{5.19}$$

To facilitate the presentation below, we denote $(\tilde{u}_N^n,\tilde{v}_N^n)\in\mathcal{B}^N$ as the continuous version of the numerical solution $\tilde{u}^n$ and $\tilde{v}^n$, respectively, with the interpolation formula given by (2.8). Similar continuous extensions could be made to obtain $\tilde{u}_N^{n*}$, $\tilde{v}_N^{n*}$, $\tilde{u}_N^{n,(1)}$, $\tilde{v}_N^{n,(1)}$, $(\tilde{u}_i)_N$, $(\tilde{v}_i)_N\in\mathcal{B}^N$.

The following preliminary estimate will be used in later analysis. Again, we assume the initial value $v^0(x)=u_t(x,t=0)\equiv 0$. The general case can be analyzed in the same manner, with more details involved.

Lemma 5.1. *At any time step t^k, $k\ge 0$, we have*

$$\|\tilde{u}_N^k\|_{H^2}\le C\left(\|D_N^2\tilde{u}^k\|_2+h^m\right). \tag{5.20}$$

Proof. Since U_i, $0\le i\le 2N$, is the interpolation of the exact solution, the following estimate is valid:

$$\overline{U^k}=\int_\Omega \mathcal{I}_N U(\cdot,t^k)\,dx=\int_\Omega U^0\,dx+O(h^m)=\bar{C}_0+O(h^m), \tag{5.21}$$

in which the interpolation approximation estimate (2.9) was applied in the second step, and the mass conservation (3.28) for the exact solution U was recalled in the last step. On the other hand, at the initial time step, a similar interpolation approximation estimate indicates that

$$\int_\Omega U^0\,dx=\int_\Omega \mathcal{I}_N U^0\,dx+O(h^m)=\overline{U^0}+O(h^m)=\overline{u^0}+O(h^m)=\beta_0+O(h^m). \tag{5.22}$$

In turn, a combination of (5.21) and (5.22) yields

$$\overline{U^k}=\int_\Omega U_N^k\,dx=\beta_0+O(h^m),\quad \forall k\ge 0. \tag{5.23}$$

In comparison with (3.29), the discrete mass conservative property for the numerical scheme, we arrive at an $O(h^m)$ order average for the numerical error function at each time step:

$$\overline{\tilde{u}^k}=\overline{U^k-u^k}=\overline{U^k}-\overline{u^k}=O(h^m),\quad \forall k\ge 0. \tag{5.24}$$

This is equivalent to

$$\int_\Omega \tilde{u}_N^k\,dx=\overline{\tilde{u}^k}=O(h^m),\quad \forall k\ge 0, \tag{5.25}$$

with the first step based on the fact that $\tilde{u}_N^k\in\mathcal{B}^N$. As an application of elliptic regularity, we arrive at

$$\|\tilde{u}_N^k\|_{H^2} \le C\left(\left\|\partial_x^2\tilde{u}_N^k\right\| + \int_\Omega \tilde{u}_N^k\,dx\right) \le C\left(\left\|D_N^2\tilde{u}^k\right\|_2 + h^m\right), \tag{5.26}$$

in which the fact that $\tilde{u}_N^k \in \mathcal{B}^N$ was used in the last step. This finishes the proof of Lemma 5.1. □

Next, we proceed into the detailed proof of Theorem 3.3, the main result of this paper.
Subtracting (3.18), (3.19)–(3.21), (3.27) from (4.3), (4.4)–(4.6), (4.14)–(4.15) yields the following system

$$\frac{\tilde{u}^{n,(1)} - \tilde{u}^n}{\Delta t} = 0, \tag{5.27}$$

$$\frac{\tilde{v}^{n,(1)} - \tilde{v}^n}{\Delta t} = \frac{1}{2}D_N^2\left(((U^n)^p) - ((u^n)^p)\right), \tag{5.28}$$

$$\partial_t\tilde{u}_2 = \tilde{v}_2, \quad \text{over } (t^n, t^{n+1}), \tag{5.29}$$

$$\partial_t\tilde{v}_2 = -D_N^4\tilde{u}_2 + D_N^2\tilde{u}_2, \quad \text{over } (t^n, t^{n+1}), \tag{5.30}$$

$$\tilde{u}_2(t^n) = \tilde{u}^{n,(1)}, \quad \tilde{v}_2(t^n) = \tilde{v}^{n,(1)}, \quad \tilde{u}_2(t^{n+1}) = \tilde{u}^{n*}, \quad \tilde{v}_2(t^{n+1}) = \tilde{v}^{n*}, \tag{5.31}$$

$$\frac{\tilde{u}^{n+1} - \tilde{u}^{n*}}{\Delta t} = \tau_1^n, \tag{5.32}$$

$$\frac{\tilde{v}^{n+1} - \tilde{v}^{n*}}{\Delta t} = \frac{1}{2}D_N^2\left(((U^{n*})^p) - ((u^{n*})^p)\right) + \tau_2^n. \tag{5.33}$$

We note a discrete $W^{2,\infty}$ bound for the exact solution

$$\|U_N\|_{L^\infty(0,T^*;W^{2,\infty})} \le C^*, \quad \text{i.e. } \left\|U_N^n\right\|_{L^\infty} \le C^*, \left\|(U_N)_x^n\right\|_{L^\infty} \le C^*, \left\|(U_N)_{xx}^n\right\|_{L^\infty} \le C^*, \tag{5.34}$$

for any $n \ge 0$, in which U_N is the continuous version of the interpolation for the exact solution. This estimate comes from the regularity of the exact solution.

An a-priori assumption up to time step t^n. We also assume a-priori that the numerical error function (for (u, v)) has an H^2 bound at time step t^n:

$$\left\|(\tilde{u}_N^n, \tilde{v}_N^n)\right\|_E^2 = \left\|(\tilde{u}_N)_x^n\right\|^2 + \left\|(\tilde{u}_N)_{xx}^n\right\|^2 + \left\|\tilde{v}_N^n\right\|^2 \le 1, \tag{5.35}$$

so that the H^2 and $W^{1,\infty}$ bounds for the numerical solution u^n are available

$$\begin{aligned}&\left\|u_N^n\right\|_{H^2} = \left\|U_N^n - \tilde{u}_N^n\right\|_{H^2} \le \left\|U_N^n\right\|_{H^2} + \left\|\tilde{u}_N^n\right\|_{H^2} \le C^* + 1 := \tilde{C}_0,\\ &\left\|u_N^n\right\|_{W^{1,\infty}} \le C\left\|u_N^n\right\|_{H^2} \le C\tilde{C}_0 := \tilde{C}_1,\end{aligned} \tag{5.36}$$

with a 1-D Sobolev embedding applied at the final step. This assumption will be recovered later.

For the numerical error evolutionary equation (5.27), its discrete inner product with $2D_N^4\tilde{u}^{n,(1)}$ and $-2D_N^2\tilde{u}^{n,(1)}$ gives

$$\left\|D_N^2\tilde{u}^{n,(1)}\right\|_2^2 - \left\|D_N^2\tilde{u}^n\right\|_2^2 + \left\|D_N^2(\tilde{u}^{n,(1)} - \tilde{u}^n)\right\|_2^2 = 0, \tag{5.37}$$

$$\left\|D_N\tilde{u}^{n,(1)}\right\|_2^2 - \left\|D_N\tilde{u}^n\right\|_2^2 + \left\|D_N(\tilde{u}^{n,(1)} - \tilde{u}^n)\right\|_2^2 = 0. \tag{5.38}$$

For the numerical error evolutionary equation (5.28), its discrete inner product with $2\tilde{v}^{n,(1)}$ yields

$$\left\|\tilde{v}^{n,(1)}\right\|_2^2 - \left\|\tilde{v}^n\right\|_2^2 + \left\|\tilde{v}^{n,(1)} - \tilde{v}^n\right\|_2^2 = \Delta t\left\langle D_N^2((U^n)^p - (u^n)^p), \tilde{v}^{n,(1)}\right\rangle. \tag{5.39}$$

For the nonlinear error term, we begin with an application of the aliasing error estimate (2.14) in Lemma 2.1:

$$\|D_N^2((U^n)^p - (u^n)^p)\|_2 \le \sqrt{p}\left\|((U_N^n)^p)_{xx} - ((u_N^n)^p)_{xx}\right\|, \tag{5.40}$$

due to the fact that $(U^n)^p - (u^n)^p$ is the interpolation of $(U_N^n)^p - (u_N^n)^p$, and $(U_N^n)^p$, $(u_N^n)^p \in \mathcal{B}^{pN}$. To analyze a continuous norm on the right hand side of (5.40), we make the following observation:

$$\begin{aligned}\left\|((U_N^n)^p)_{xx} - ((u_N^n)^p)_{xx}\right\| &\le C\left(\left\|U_N^n\right\|_{H^2}^{p-1} + \left\|u_N^n\right\|_{H^2}^{p-1}\right)\cdot\left\|\tilde{u}_N^n\right\|_{H^2}\\ &\le \tilde{C}_2\left\|\tilde{u}_N^n\right\|_{H^2}, \quad \text{with } \tilde{C}_2 = C\left((C^*)^{p-1} + \tilde{C}_0^{p-1}\right),\end{aligned} \tag{5.41}$$

$$\text{since } \left\|U_N^n\right\|_{H^2} \le CC^*, \quad \left\|u_N^n\right\|_{H^2} \le \tilde{C}_0, \tag{5.42}$$

with repeated applications of 1-D Sobolev embedding. Then we obtain the following estimate

$$\begin{aligned}\left\langle D_N^2((U^n)^p-(u^n)^p),\tilde{v}^{n,(1)}\right\rangle &\le \sqrt{p}\tilde{C}_2\left\|\tilde{u}_N^n\right\|_{H^2}\cdot\left\|\tilde{v}^{n,(1)}\right\|_2\\ &\le \frac{1}{2}\tilde{C}_3\left(\left\|\tilde{u}_N^n\right\|_{H^2}^2+\left\|\tilde{v}^{n,(1)}\right\|_2^2\right),\quad \text{with } \tilde{C}_3=\sqrt{p}\tilde{C}_2.\end{aligned}\tag{5.43}$$

Therefore, a combination of (5.37), (5.38), (5.39) and (5.43) leads to

$$\begin{aligned}\left\|(\tilde{u}^{n,(1)},\tilde{v}^{n,(1)})\right\|_E^2-\left\|(\tilde{u}^n,\tilde{v}^n)\right\|_E^2 &\le \frac{\tilde{C}_3}{2}\Delta t\left(\left\|\tilde{u}_N^n\right\|_{H^2}^2+\left\|\tilde{v}^{n,(1)}\right\|_2^2\right)\\ &\le \frac{\tilde{C}_3}{2}\Delta t\left(\left\|(\tilde{u}^{n,(1)},\tilde{v}^{n,(1)})\right\|_E^2+\left\|(\tilde{u}^n,\tilde{v}^n)\right\|_E^2+h^{2m}\right),\end{aligned}\tag{5.44}$$

in which the last step was based on the fact that $\left\|D_N^2\tilde{u}_N^n\right\|^2$ and $\left\|\tilde{v}^{n,(1)}\right\|_2^2$ could be absorbed into $\left\|(\tilde{u}^n,\tilde{v}^n)\right\|_E^2$, $\left\|(\tilde{u}^{n,(1)},\tilde{v}^{n,(1)})\right\|_E^2$, respectively, and the preliminary estimate (5.20) was also applied. Moreover, it is observed that (5.44) could be further refined as

$$\left\|(\tilde{u}^{n,(1)},\tilde{v}^{n,(1)})\right\|_E^2-\left\|(\tilde{u}^n,\tilde{v}^n)\right\|_E^2\le\tilde{C}_4\Delta t(\left\|(\tilde{u}^n,\tilde{v}^n)\right\|_E^2+h^{2m}),\quad \text{with } \tilde{C}_4 \text{ dependent on } \tilde{C}_3.\tag{5.45}$$

For the numerical error evolutionary equation (5.29)–(5.31) in the second stage, an energy estimate for the linear wave equation implies that

$$\begin{aligned}\left\|(\tilde{u}^{n*},\tilde{v}^{n*})\right\|_E^2&=\left\|D_N\tilde{u}^{n*}\right\|_2^2+\left\|D_N^2\tilde{u}^{n*}\right\|_2^2+\left\|\tilde{v}^{n*}\right\|_2^2\\ &=\left\|(\tilde{u}^{n,(1)},\tilde{v}^{n,(1)})\right\|_E^2=\left\|D_N\tilde{u}^{n,(1)}\right\|_2^2+\left\|D_N^2\tilde{u}^{n,(1)}\right\|_2^2+\left\|\tilde{v}^{n,(1)}\right\|_2^2.\end{aligned}\tag{5.46}$$

Next, we analyze the numerical error equation (5.32)–(5.33). Taking a discrete inner product with (5.32) by $2D_N^4\tilde{u}^{n+1}$, $-2D_N^2\tilde{u}^{n+1}$, results in

$$\left\|D_N^2\tilde{u}^{n+1}\right\|_2^2-\left\|D_N^2\tilde{u}^{n*}\right\|_2^2+\left\|D_N^2(\tilde{u}^{n+1}-\tilde{u}^{n*})\right\|_2^2\le\Delta t\left\|D_N^2\tau_1^n\right\|_2^2+\Delta t\left\|D_N^2\tilde{u}^{n+1}\right\|_2^2,\tag{5.47}$$

$$\left\|D_N\tilde{u}^{n+1}\right\|_2^2-\left\|D_N\tilde{u}^{n*}\right\|_2^2+\left\|D_N(\tilde{u}^{n+1}-\tilde{u}^{n*})\right\|_2^2\le\Delta t\left\|D_N\tau_1^n\right\|_2^2+\Delta t\left\|D_N\tilde{u}^{n+1}\right\|_2^2.\tag{5.48}$$

Taking an inner product with (5.33) by the error function $2\tilde{v}^{n+1}$ gives

$$\begin{aligned}&\left\|\tilde{v}^{n+1}\right\|_2^2-\left\|\tilde{v}^{n*}\right\|_2^2+\left\|\tilde{v}^{n+1}-\tilde{v}^{n*}\right\|_2^2\\ &=\Delta t\left\langle D_N^2((U^{n*})^p-(u^{n*})^p),\tilde{v}^{n+1}\right\rangle+2\Delta t\left\langle\tau_2^n,\tilde{v}^{n+1}\right\rangle,\end{aligned}\tag{5.49}$$

$$\text{with } 2\left\langle\tau_2^n,\tilde{v}^{n+1}\right\rangle\le\left\|\tau_2^n\right\|_2^2+\left\|\tilde{v}^{n+1}\right\|_2^2.\tag{5.50}$$

To bound the nonlinear error term, we have a similar estimate as (5.40):

$$\|D_N^2((U^{n*})^p-(u^{n*})^p)\|_2\le\sqrt{p}\left\|((U_N^{n*})^p)_{xx}-((u_N^{n*})^p)_{xx}\right\|.\tag{5.51}$$

In addition, repeated applications of 1-D Sobolev embedding leads to

$$\left\|((U_N^{n*})^p)_{xx}-((u_N^{n*})^p)_{xx}\right\|\le C\left(\left\|U_N^{n*}\right\|_{H^2}^{p-1}+\left\|u_N^{n*}\right\|_{H^2}^{p-1}\right)\cdot\left\|\tilde{u}_N^{n*}\right\|_{H^2}.\tag{5.52}$$

For U_N^{n*}, the following estimate is valid:

$$\left\|U_N^{n*}-\frac{1}{L}\int_\Omega U_N^{n*}\,dx\right\|_{H^2}^2\le\left\|(U^{n*},V^{n*})\right\|_E^2=\left\|(U^n,V^n)\right\|_E^2\le C(C^*)^2,\tag{5.53}$$

in which the energy conservation between (U^{n*},V^{n*}) and (U^n,V^n) was applied in the second step. Meanwhile, we have $\int_\Omega U_N^{n*}\,dx=\int_\Omega U_N^n\,dx=\beta_0+O(h^m)$, by (5.23). This in turn implies that

$$\left\|U_N^{n*}\right\|_{H^2}\le C\left(C^*+|\beta_0|+h^m\right).\tag{5.54}$$

For u_N^{n*}, the following estimate could be derived, in a similar fashion as (5.36):

$$\begin{aligned}\left\|u_N^{n*}\right\|_{H^2} &= \left\|U_N^{n*}-\tilde{u}_N^{n*}\right\|_{H^2} \le \left\|U_N^{n*}\right\|_{H^2}+\left\|\tilde{u}_N^{n*}\right\|_{H^2} \le \left\|U_N^{n*}\right\|_{H^2}+\left\|\tilde{u}^{n*}\right\|_E + Ch^m \\ &\le \left\|U_N^{n*}\right\|_{H^2}+\left\|\tilde{u}^{n}\right\|_E + Ch^m \le C\left(C^*+|\beta_0|+1\right),\end{aligned} \tag{5.55}$$

in which the energy conservation $\left\|\tilde{u}^{n*}\right\|_E = \left\|\tilde{u}^{n}\right\|_E$ was applied in the fourth step. Then we arrive at

$$\left\|((U_N^{n*})^p)_{xx}-((u_N^{n*})^p)_{xx}\right\| \le \tilde{C}_5\left\|\tilde{u}_N^{n*}\right\|_{H^2}, \quad \text{with } \tilde{C}_5 = C\left((C^*)^{p-1}+|\beta_0|^{p-1}+1\right), \tag{5.56}$$

which in turn leads to the following estimate

$$\left\langle D_N^2((U^{n*})^p-(u^{n*})^p),\tilde{v}^{n+1}\right\rangle \le \sqrt{p}\tilde{C}_5\left\|\tilde{u}_N^{n*}\right\|_{H^2}\cdot\left\|\tilde{v}^{n+1}\right\|_2 \le \frac{\tilde{C}_6}{2}\left(\left\|\tilde{u}_N^{n*}\right\|_{H^2}^2+\left\|\tilde{v}^{n+1}\right\|_2^2\right), \tag{5.57}$$

with $\tilde{C}_6=\sqrt{p}\tilde{C}_5$. Going back to (5.49), (5.50), we arrive at

$$\left\|\tilde{v}^{n+1}\right\|_2^2-\left\|\tilde{v}^{n*}\right\|_2^2 \le \frac{\tilde{C}_6}{2}\Delta t\left\|\tilde{u}_N^{n*}\right\|_{H^2}^2+\Delta t\left(\frac{\tilde{C}_6}{2}+1\right)\left\|\tilde{v}^{n+1}\right\|_2^2+\Delta t\left\|\tau_2^n\right\|_2^2. \tag{5.58}$$

Moreover, its combination with (5.47) and (5.48) yields

$$\begin{aligned}&\left\|(\tilde{u}^{n+1},\tilde{v}^{n+1})\right\|_E^2-\left\|(\tilde{u}^{n*},\tilde{v}^{n*})\right\|_E^2 \\ &\le \Delta t\left(\left\|D_N^2\tilde{u}^{n+1}\right\|_2^2+\left\|D_N\tilde{u}^{n+1}\right\|_2^2+\frac{\tilde{C}_6}{2}\left\|\tilde{u}_N^{n*}\right\|_{H^2}^2+(\frac{\tilde{C}_6}{2}+1)\left\|\tilde{v}^{n+1}\right\|_2^2\right) \\ &\quad+\Delta t\left(\left\|\tau_1^n\right\|_{H_h^2}^2+\left\|\tau_2^n\right\|_2^2\right).\end{aligned} \tag{5.59}$$

As a consequence, a combination of (5.45), (5.46) and (5.59) results in

$$\begin{aligned}&\left\|(\tilde{u}^{n+1},\tilde{v}^{n+1})\right\|_E^2-\left\|(\tilde{u}^{n},\tilde{v}^{n})\right\|_E^2 \\ &\le \tilde{C}_4\Delta t\left\|(\tilde{u}^{n},\tilde{v}^{n})\right\|_E^2+\Delta t\left(\left\|D_N^2\tilde{u}^{n+1}\right\|_2^2+\left\|D_N\tilde{u}^{n+1}\right\|_2^2+\frac{\tilde{C}_6}{2}\left\|\tilde{u}_N^{n*}\right\|_{H^2}^2+(\frac{\tilde{C}_6}{2}+1)\left\|\tilde{v}^{n+1}\right\|_2^2\right) \\ &\quad+\Delta t\left(\left\|\tau_1^n\right\|_{H^2}^2+\left\|\tau_2^n\right\|_2^2+h^{2m}\right) \\ &\le \tilde{C}_4\Delta t\left\|(\tilde{u}^{n},\tilde{v}^{n})\right\|_E^2+(\frac{\tilde{C}_6}{2}+1)\Delta t\left\|(\tilde{u}^{n+1},\tilde{v}^{n+1})\right\|_E^2+\frac{\tilde{C}_6}{2}\left\|\tilde{u}_N^{n*}\right\|_{H^2}^2 \\ &\quad+\Delta t\left(\left\|\tau_1^n\right\|_{H_h^2}^2+\left\|\tau_2^n\right\|_2^2+h^{2m}\right) \\ &\le \tilde{C}_7\Delta t\left\|(\tilde{u}^{n},\tilde{v}^{n})\right\|_E^2+(\frac{\tilde{C}_6}{2}+1)\Delta t\left\|(\tilde{u}^{n+1},\tilde{v}^{n+1})\right\|_E^2+\Delta t\left(\left\|\tau_1^n\right\|_{H_h^2}^2+\left\|\tau_2^n\right\|_2^2+h^{2m}\right),\end{aligned} \tag{5.60}$$

with the preliminary estimates (5.20), (5.45), (5.46) repeatedly recalled. Meanwhile, since the $\|\cdot\|_E$ norm of the numerical error function at time step t^{n+1} has been involved on the right hand side of (5.60), an upper bound for the time step size is needed to pass through the analysis. Under the constraint

$$(\frac{\tilde{C}_6}{2}+1)\Delta t \le \frac{1}{2}, \quad \text{so that } \frac{1}{1-(\frac{\tilde{C}_6}{2}+1)\Delta t} \le 1+2(\frac{\tilde{C}_6}{2}+1)\Delta t = 1+(\tilde{C}_6+2)\Delta t, \tag{5.61}$$

we have

$$\begin{aligned}\left\|(\tilde{u}^{n+1},\tilde{v}^{n+1})\right\|_E^2 &\le \mathrm{e}^{(\tilde{C}_7+\tilde{C}_6+2)\Delta t}\left\|(\tilde{u}^{n},\tilde{v}^{n})\right\|_E^2 \\ &\quad+\Delta t\left(1+(\tilde{C}_6+2)\Delta t\right)\left(\left\|\tau_1^n\right\|_{H_h^2}^2+\left\|\tau_2^n\right\|_2^2+h^{2m}\right),\end{aligned} \tag{5.62}$$

in which the following inequalities are recalled:

$$1+\tilde{C}_7\Delta t \le \mathrm{e}^{\tilde{C}_7\Delta t}, \quad 1+(\tilde{C}_6+2)\Delta t \le \mathrm{e}^{(\tilde{C}_6+2)\Delta t}. \tag{5.63}$$

It is observed that the upper bound for Δt given by (5.61), i.e., $\Delta t \le \frac{1}{\tilde{C}_6+2}$, is not a severe constraint, since $\tilde{C}_6 = O(1)$. In turn, an application of the discrete Gronwall inequality indicates that

$$\left\|(\tilde{u}^{n+1}, \tilde{v}^{n+1})\right\|_E \le \tilde{C}_8(\Delta t^2 + h^m), \tag{5.64}$$

with $\tilde{C}_8$ dependent on $\tilde{C}_6$, $\tilde{C}_7$ and T^*, independent of Δt and h. Note that the local truncation error estimate, $\left\|\tau_1^n\right\|_{H^2}$, $\|\tau_2\|_2 \le C_0(\Delta t^2 + h^m)$, has been used. In turn, an application of the preliminary inequality (5.20) (given by Lemma 5.1) results in the desired convergence estimate (3.41).

Recovery of the a-priori bound (5.35). With the help of the error estimate (5.64), $\ell^\infty(0, T; H^2)$ for variable u and $\ell^\infty(0, T; L^2)$ for variable v, we see that the a-priori bound (5.35) is also valid for the numerical error function $(\tilde{u}, \tilde{v})$ at time step t^{n+1}, provided that

$$\Delta t \le \left(2\tilde{C}_8\right)^{-1/2}, \quad h \le \left(2\tilde{C}_8\right)^{-1/m}, \quad \text{with } \tilde{C}_8 \text{ dependent on } T^*.$$

This completes the second order convergence analysis, $\ell^\infty(0, T^*; H^2)$ for u, and $\ell^\infty(0, T^*; L^2)$ for v.

Remark 5.2. A severe stability condition $\Delta t \le Ch^2$ reported in the earlier work [16] is more associated with a theoretical analysis difficulty than an essential constraint in practical computations. In fact, for the following linear scheme, which corresponds to the linear part and the fourth order diffusion of the numerical method studied in [16]:

$$\frac{u^{n+1} - 2u^n + u^{n-1}}{\Delta t^2} = -\frac{1}{4} D_N^4 \left(u^{n+1} + 2u^n + u^{n-1}\right), \tag{5.65}$$

a careful estimate shows its unconditional stability, by taking inner product by $u^{n+1} - u^{n-1}$. Also see the related analysis by Dupont [20].

However, due to certain technical difficulties, for its combination with the nonlinear term, the stability and convergence could only be justified under a severe constraint $\Delta t = O(h^2)$. This technical difficulty may be able to be overcome, and the authors will consider this analysis in the future.

Remark 5.3. In a more recent work [13], an alternative second order temporal approximation was proposed and analyzed, with an intermediate variable to approximate $v = u_t$ introduced in the numerical scheme. The convergence analysis in the stronger energy norm was established without the time step restriction $\Delta t \le Ch^2$, using similar techniques presented in this article.

6. Numerical results

In this section we present a numerical experiment for the second order operator splitting scheme (3.15)–(3.26). Similar to [13,16], we take $p = 2$, and the exact solitary wave solution of the GB equation is given by

$$u_e(x, t) = -A\,\mathrm{sech}^2\left(\frac{P}{2}(x - c_0 t)\right), \tag{6.1}$$

with $0 < P \le 1$. The amplitude A, the wave speed c_0 and the real parameter P have to satisfy

$$A = \frac{3P^2}{2}, \quad c_0 = \left(1 - P^2\right)^{1/2}. \tag{6.2}$$

The Fourier pseudo-spectral approximation on an interval $(-L, L)$, with L large enough, is a natural choice, since the exact profile (6.1) decays exponentially as $|x| \to \infty$. We set the computational domain as $\Omega = (-80, 80)$, and a moderate amplitude $A = 0.5$ is taken.

A comparison between the numerical solution and the exact solution of u at a final time $T = 4$ is displayed in Fig. 1; the time step is taken as $\Delta t = 2 \times 10^{-4}$, and the spatial resolution is given by $N = 128$. A very good match is clearly demonstrated in this figure.

6.1. Spectral convergence in space

To investigate the accuracy in space, we fix $\Delta t = 10^{-4}$ and compute solutions with grid sizes $N = 32$ to $N = 160$ in increments of 8. For this fixed time step size, the temporal numerical error becomes negligible. The following numerical errors at the final time $T = 4$

$$\|v - v_e\|_2, \quad \text{and} \quad \left\|D_N^2(u - u_e)\right\|_2, \tag{6.3}$$

are presented in Fig. 2. The spatial spectral accuracy is apparently observed for both u and $v = u_t$. And also, a saturation of spectral accuracy appears with an increasing N, since the numerical error is dominated by the temporal one for $N \ge 128$.

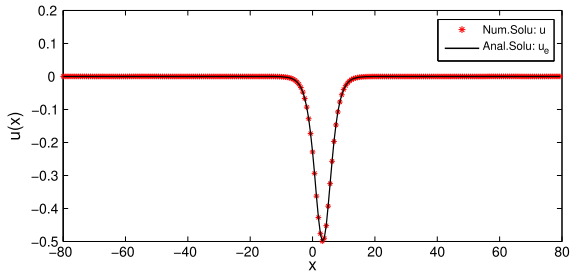

Fig. 1. A comparison between the numerical solution and the exact solution. The solid line represents the plot for the exact profile (6.1) at $T = 4.0$, while the star line stands for that of the numerical solution, computed by the second order operator splitting scheme (3.15)–(3.26). The time step size is chosen as $\Delta t = 2 \times 10^{-4}$, and the spatial resolution is given by $N = 128$.

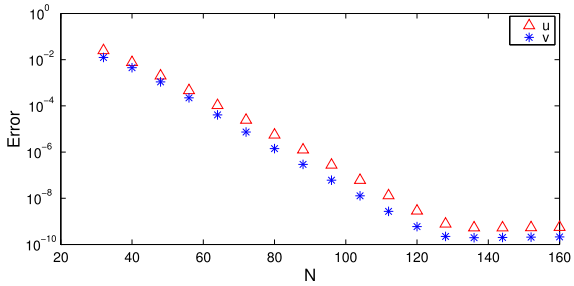

Fig. 2. Discrete L^2 numerical errors for $v = u_t$ and H^2 numerical errors for u at $T = 4.0$, plotted versus N, the number of spatial grid point, for the second order operator splitting scheme (3.15)–(3.26). The time step size is fixed as $\Delta t = 10^{-4}$. An apparent spatial spectral accuracy is observed for both variables.

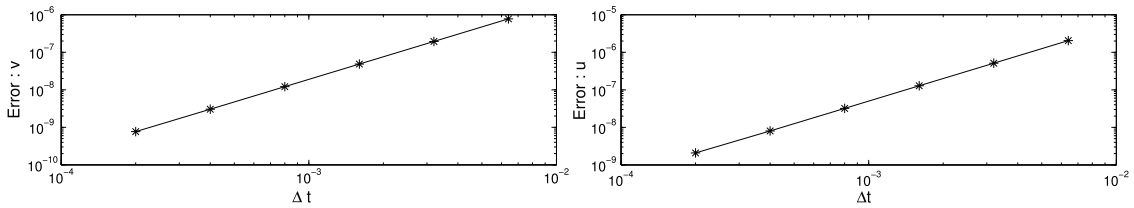

Fig. 3. Discrete L^2 numerical errors for $v = u_t$ and H^2 numerical errors for u at $T = 4.0$, plotted versus Δt, the time step size, for the second order operator splitting scheme (3.15)–(3.26). The spatial resolution is fixed as $N = 128$. The data lie roughly on curves $C\Delta t^2$, for appropriate choices of C, confirming the full second-order temporal accuracy.

6.2. Second order convergence in time

To study the temporal accuracy, we fix the spatial resolution as $N = 128$ so that the spatial discretization error is negligible and the numerical error is dominated by the temporal ones. We compute solutions with a sequence of time step sizes, $\Delta t = \Delta t_0/2^K$, with $\Delta t_0 = 6.4 \times 10^{-3}$ and $0 \le K \le 6$. The discrete L^2 and H^2 norms of the numerical errors, for both $v = u_t$ and u, are reported in Fig. 3. A clear second order accuracy is observed for both variables.

7. Concluding remarks

In this article, we analyze a second order operator splitting scheme for the GB equation (1.1), with Fourier pseudo-spectral approximation in space. A rewritten form of a system of two equations, for the original variable u and $v = u_t$, respectively, is used to facilitate the numerical design. Subsequently, the nonlinear stability and convergence analysis are provided in detail. A careful Taylor expansion for both the exact solution and the constructed approximate solution results in the second order truncation error in time, and the standard approximation estimate in pseudo-spectral space implies the spectral accuracy in space. In addition, with the help of an a-priori H^2 assumption for the numerical solution at the previous time step and an aliasing error control technique, we perform a linearized stability analysis for the numerical error function and obtain the convergence estimate in the energy norm: an $\ell^\infty(0, T^*; H^2)$ convergence for u and $\ell^\infty(0, T^*; \ell^2)$ convergence for $v = u_t$. And also, the presented convergence is unconditional for the time step in terms of the spatial grid size, in comparison with a severe time step restriction, $\Delta t \le Ch^2$, required in many existing works. A simple numerical experiment also verifies the unconditional convergence, second order accuracy in time, and spectral accuracy in space.

Acknowledgements

This work is supported in part by NSF DMS-1217080 (J. Huang), NSF DMS-1418689 (C. Wang) and NSFC 11271281 (X. Yue).

References

[1] B.S. Attili, The Adomian decomposition method for solving the Boussinesq equation arising in water wave propagation, Numer. Methods Partial Differ. Equ. 22 (2006) 1337–1347.
[2] S. Badia, R. Planas, J.V. Gutiérrez-Santacreu, Unconditionally stable operator splitting algorithms for the incompressible magnetohydrodynamics system discretized by a stabilized finite element formulation based on projections, Int. J. Numer. Methods Eng. 93 (2013) 302–328.
[3] W. Bao, S. Jin, P. Markowich, On time-splitting spectral approximations for the Schrödinger equation in the semiclassical regime, J. Comput. Phys. 175 (2002) 487–524.
[4] A. Bátkai, P. Csomós, B. Farkas, Operator splitting for nonautonomous delay equations, Comput. Math. Appl. 65 (2013) 315–324.
[5] A. Bátkai, P. Csomós, B. Farkas, Operator splitting for dissipative delay equations, Proc. Appl. Math. Mech. 14 (2013) 989–990.
[6] J. Boyd, Chebyshev and Fourier Spectral Methods, 2nd edition, Dover, New York, NY, 2001.
[7] A.G. Bratsos, A second order numerical scheme for the improved Boussinesq equation, Phys. Lett. A 370 (2007) 145–147.
[8] A.G. Bratsos, A predictor–corrector scheme for the improved Boussinesq equation, Chaos Solitons Fractals 40 (2009) 2083–2094.
[9] A. Bressan, A. Quarteroni, An implicit/explicit spectral method for Burgers' equation, Calcolo 23 (3) (1986) 265–284.
[10] C. Canuto, A. Quarteroni, Approximation results for orthogonal polynomials in Sobolev spaces, Math. Comput. 38 (1982) 67–86.
[11] C. Canuto, M.Y. Hussani, A. Quarteroni, T.A. Zang, Spectral Methods: Evolution to Complex Geometries and Applications to Fluid Dynamics, Springer-Verlag, Berlin, 2007.
[12] G.Q. Chen, Q. Du, E. Tadmor, Super viscosity approximations to multi-dimensional scalar conservation laws, Math. Comput. 61 (204) (1993) 629–643.
[13] K. Cheng, W. Feng, C. Wang, S. Wise, A Fourier pseudospectral method for the "Good" Boussinesq equation with second-order temporal accuracy, Numer. Methods Partial Differ. Equ. 31 (2015) 202–224.
[14] R. Cienfuegos, E. Barthélemy, P. Bonneton, A fourth-order compact finite volume scheme for fully nonlinear and weakly dispersive Boussinesq-type equations. Part I: model development and analysis, Int. J. Numer. Methods Fluids 51 (2006) 1217–1253.
[15] R. Cienfuegos, E. Barthélemy, P. Bonneton, A fourth-order compact finite volume scheme for fully nonlinear and weakly dispersive Boussinesq-type equations. Part II: boundary conditions and validation, Int. J. Numer. Methods Fluids 53 (2007) 1423–1455.
[16] J. De Frutos, T. Ortega, J.M. Sanz-Serna, Pseudospectral method for the "good" Boussinesq equation, Math. Comput. 57 (1991) 109–122.
[17] Z. Deng, H. Ma, Error estimate of the Fourier collocation method for the Benjamin–Ono equation, Numer. Math., Theory Methods Appl. 2 (2009) 341–352.
[18] Z. Deng, H. Ma, Optimal error estimates of the Fourier spectral method for a class of nonlocal, nonlinear dispersive wave equations, Appl. Numer. Math. 59 (2009) 988–1010.
[19] Q. Du, B. Guo, J. Shen, Fourier spectral approximation to a dissipative system modeling the flow of liquid crystals, SIAM J. Numer. Anal. 39 (3) (2001) 735–762.
[20] T. Dupont, Galerkin methods for first order hyperbolics: an example, SIAM J. Numer. Anal. 10 (2009) 890–899.
[21] W. E, Convergence of spectral methods for the Burgers' equation, SIAM J. Numer. Anal. 29 (6) (1992) 1520–1541.
[22] W. E, Convergence of Fourier methods for Navier–Stokes equations, SIAM J. Numer. Anal. 30 (3) (1993) 650–674.
[23] L. Einkemmer, A. Ostermann, An almost symmetric Strang splitting scheme for nonlinear evolution equations, Comput. Math. Appl. 67 (2014) 2144–2157.
[24] L. Einkemmer, A. Ostermann, Convergence analysis of Strang splitting for Vlasov-type equations, SIAM J. Numer. Anal. 52 (2014) 140–155.
[25] L. Farah, M. Scialom, On the periodic "good" Boussinesq equation, Proc. Am. Math. Soc. 138 (3) (2010) 953–964.
[26] D. Gottlieb, S.A. Orszag, Numerical Analysis of Spectral Methods, Theory and Applications, SIAM, Philadelphia, PA, 1977.
[27] S. Gottlieb, C. Wang, Stability and convergence analysis of fully discrete Fourier collocation spectral method for 3-D viscous Burgers' Equation, J. Sci. Comput. 53 (2012) 102–128.
[28] B.Y. Guo, A spectral method for the vorticity equation on the surface, Math. Comput. 64 (211) (1995) 1067–1069.
[29] B.Y. Guo, H.P. Ma, E. Tadmor, Spectral vanishing viscosity method for nonlinear conservation laws, SIAM J. Numer. Anal. 39 (2001) 1254–1268.
[30] B.Y. Guo, J. Zou, Fourier spectral projection method and nonlinear convergence analysis for Navier–Stokes equations, J. Math. Anal. Appl. 282 (2) (2003) 766–791.
[31] J. Hesthaven, S. Gottlieb, D. Gottlieb, Spectral Methods for Time-Dependent Problems, Cambridge University Press, Cambridge, 2007.
[32] O. Karakashian, Y. Xing, A posteriori error estimate for conservative local discontinuous Galerkin methods for the generalized Korteweg–de Vries equation, Commun. Comput. Phys. 20 (1) (2016) 250–278.
[33] M. Koleva, L. Vulkov, Operator splitting kernel based numerical method for a generalized Leland's model, J. Comput. Appl. Math. 275 (2015) 294–303.
[34] H.G. Lee, J.Y. Lee, A second order operator splitting method for Allen–Cahn type equations with nonlinear source terms, Phys. A 432 (2015) 24–34.
[35] D. Levy, C.-W. Shu, J. Yan, Local discontinuous Galerkin methods for nonlinear dispersive equations, J. Comput. Phys. 196 (2004) 751–772.
[36] X. Li, Z. Qiao, H. Zhang, Convergence of a fast explicit operator splitting method for the epitaxial growth model with slope selection, SIAM J. Numer. Anal. 55 (1) (2017) 265–285.
[37] F. Linares, M. Scialom, Asymptotic behavior of solutions of a generalized Boussinesq type equation, Nonlinear Anal., Theory Methods Appl. 25 (11) (1995) 1147–1158.
[38] J.C. López-Marcos, J.M. Sanz-Serna, Stability and convergence in numerical analysis. III: linear investigation of nonlinear stability, IMA J. Numer. Anal. 7 (1988) 71–84.
[39] C. Lubich, On splitting methods for Schrödinger–Poisson and cubic nonlinear Schrödinger equations, Math. Comput. 77 (264) (2008) 2141–2153.
[40] Y. Maday, A. Quarteroni, Legendre and Chebyshev spectral approximations of Burgers' equation, Numer. Math. 37 (1981) 321–332.
[41] Y. Maday, A. Quarteroni, Approximation of Burgers' equation by pseudospectral methods, RAIRO. Anal. Numér. 16 (1982) 375–404.
[42] Y. Maday, A. Quarteroni, Spectral and pseudospectral approximation to Navier–Stokes equations, SIAM J. Numer. Anal. 19 (4) (1982) 761–780.
[43] Y. Maday, A. Quarteroni, Error analysis for spectral approximation of the Korteweg–de Vries equation, Math. Model. Numer. Anal. 22 (1988) 499–529.
[44] Y. Maday, S.M. Ould Kaber, E. Tadmor, Legendre pseudospectral viscosity method for nonlinear conservation laws, SIAM J. Numer. Anal. 30 (2) (1993) 321–342.
[45] A. Majda, J. McDonough, S. Osher, The Fourier method for non-smooth initial data, Math. Comput. 32 (1978) 1041–1081.
[46] V.S. Manotanjan, A.R. Mitchell, J.L. Morris, Numerical solutions of the good Boussinesq equation, SIAM J. Sci. Stat. Comput. 5 (1984) 946–957.
[47] V.S. Manotanjan, T. Ortega, J.M. Sanz-Serna, Soliton and antisoliton interactions in the "good" Boussinesq equation, J. Math. Phys. 29 (1988) 1964–1968.
[48] S. Oh, A. Stefanov, Improved local well-posedness for the periodic "good" Boussinesq equation, J. Differ. Equ. 254 (10) (2013) 4047–4065.

[49] T. Ortega, J.M. Sanz-Serna, Nonlinear stability and convergence of finite difference methods for the "good" Boussinesq equation, Numer. Math. 58 (1990) 215–229.
[50] A.K. Pani, H. Saranga, Finite element Galerkin method for the "good" Boussinesq equation, Nonlinear Anal. 29 (1997) 937–956.
[51] R. Pego, M. Weinstein, Convective linear stability of solitary waves for Boussinesq equations, Stud. Appl. Math. 99 (4) (1997) 311–375.
[52] B. Pelloni, V.A. Dougalis, Error estimates for a fully discrete spectral scheme for a class of nonlinear, nonlocal dispersive wave equations, Appl. Numer. Math. 37 (2001) 95–107.
[53] J. Shen, Z.Q. Wang, Error analysis of the Strang time-splitting Laguerre–Hermite/Hermite collocation methods for the Gross–Pitaevskii equation, Found. Comput. Math. 13 (2013) 99–137.
[54] E. Tadmor, The exponential accuracy of Fourier and Chebyshev differencing methods, SIAM J. Numer. Anal. 23 (1986) 1–10.
[55] E. Tadmor, Convergence of spectral methods to nonlinear conservation laws, SIAM J. Numer. Anal. 26 (1) (1989) 30–44.
[56] E. Tadmor, Shock capturing by the spectral viscosity method, Comput. Methods Appl. Mech. Eng. 80 (1990) 197–208.
[57] M. Thalhammer, Convergence analysis of high-order time-splitting pseudospectral methods for nonlinear Schrödinger equations, SIAM J. Numer. Anal. 50 (6) (2012) 3231–3258.
[58] M. Tsutsumi, T. Matahashi, On the Cauchy problem for the Boussinesq type equation, Math. Jpn. 36 (2) (1991) 371–379.
[59] Y. Xu, C.-W. Shu, Local discontinuous Galerkin methods for three classes of nonlinear wave equations, J. Comput. Math. 22 (2) (2004) 250–274.
[60] J. Yan, C.-W. Shu, A local discontinuous Galerkin method for KdV type equations, SIAM J. Numer. Anal. 40 (2002) 769–791.
[61] J. Yan, C.-W. Shu, Local discontinuous Galerkin methods for partial differential equations with higher order derivatives, J. Sci. Comput. 17 (2002) 27–47.
[62] S. Zhao, Operator splitting ADI schemes for pseudo-time coupled nonlinear solvation simulations, J. Comput. Phys. 257 (2014) 1000–1021.